

# Development of a Micro Ultrasonic Transducer

Fernando F. Dall'Agnol<sup>1</sup>\*, Antônio C. F. De Mattos<sup>1</sup>

<sup>1</sup> Center for Information Technology Renato Archer (CTI), Campinas, SP, Brazil

\*Corresponding author: Rod. Dom Pedro I km 143.6, Jd. Santa Mônica, Campinas-SP, 13069-901, email: fernando.dallagnol@cti.gov.br

## Abstract

We simulate a Capacitive Micromachined Ultrasound Transducer (CMUT) using COMSOL. The CMUT is an electromechanical system, therefore, we couple the physics of electrical and structural mechanics to describe its dynamics. We obtain the distributions of the electric field and the stress as a function of time. Finally, we derived the time evolution of the device for several frequencies, from where we obtain the maximum frequency of operation.

**Keywords:** MEMS, Ultrasound transducer.

## 1. Introduction

Capacitive Micromachined Ultrasound Transducer (CMUT)<sup>1</sup> structures are attractive sensors/actuators due to its CMOS (Complementary Metal Oxide Semiconductor)<sup>2</sup> compatible production that uses the already mature methods of integrated circuit industry in Silicon. Basically a CMUT structure comprises a capacitor where one electrode is a suspended membrane. Electrostatic forces act when a voltage is applied inducing a bending of the membrane. On the other hand, if the membrane is subjected to a pressure variation, an electric current is generated by the capacitance change when under a bias voltage. This dual action of actuation and sensing is important in highly integrated transducer design for future ultrasonic proximity sensors and imaging devices.

A CMUT is made using several microelectronic processes like vapor deposition<sup>3</sup>, etching<sup>4</sup>, liftoff<sup>5</sup>, etc. The final structure can be approximated to the CAD represented in figure 1. All geometrical parameters and materials can be varied to influence the operation of the device.

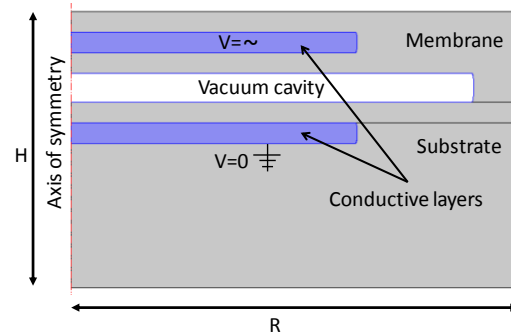


**Figure 1.** Main features of the simulated acoustic transducer. Typically  $R \gg H$ .

## 2. Use of COMSOL Multiphysics

The CMUT is modeled in Comsol as follows: layers in blue in figure 1 are conductors, where an alternating voltage is applied. This generates the driving force to oscillate the membrane and the stiffness of the materials provides the restoring force. To model the dynamics in Comsol we combine the *Electrostatics*, *Solid Mechanics* and *Moving Mesh* modules. The latter is added to have the mesh deforming with the membrane. This is necessary, because the position of the membrane will sensibly affect the electrostatic force between the membrane and the substrate. Each module has its own set of initial conditions and boundary conditions (BC). The ability to couple several physical systems is one of Comsol's characteristics we explore. The variables from one module will enter as parameters in the others.

### 2.1 Electrostatics

Figure 2 shows the domains where *Electrostatics* is applied. The bottom plate is grounded ( $V=0$ ). A voltage on the top plate is a sine function that varies in phase with the external excitation as:

$$V = V_0 \sin(2\pi f t). \quad (1)$$

There is no electric field inside the conductor, so the interior of the plates are excluded from the *Electrostatic* simulation. Therefore, equation (1) is applied only on the *Edges* of the plate.

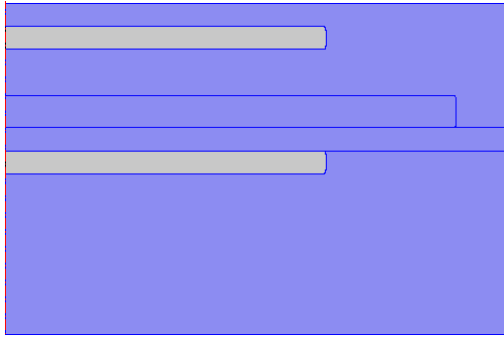


**Figure 2.** In blue, the domains where the *Electrostatics* is applied.

The electric field is expected to be confined in the plate. So, the outermost surfaces should contain no induced charge. We set this boundaries (see figure 3) as a *Zero Charge BC*. It states that the electric field must be tangential to the boundaries ( $\mathbf{D} \cdot \mathbf{n} = 0$ ), thus, no surface charge accumulates.

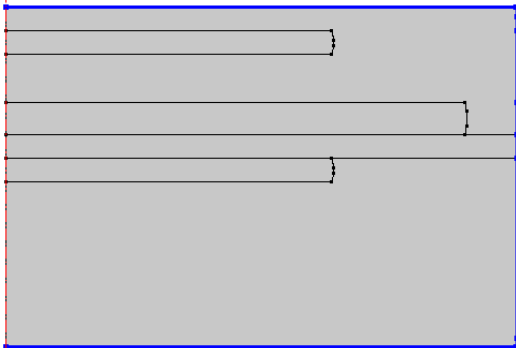


**Figure 3.** Surfaces with BC of zero charge.

The BCs determine the field distribution, which will be used to calculate the force that pulls the plates. Figures 4 and 5 show the distributions of the potential and the electric field respectively. Note in figure 5 that the field is indeed confined between the plates.

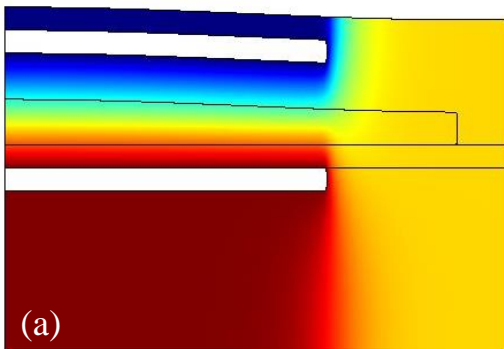


**Figure 4.** Potential distribution.

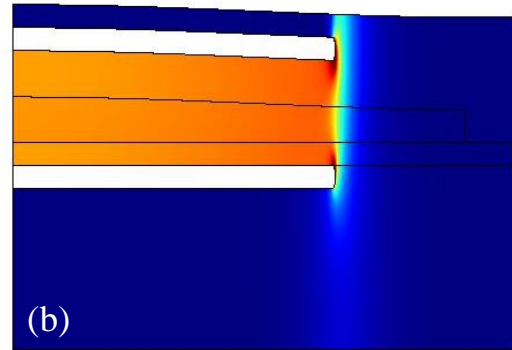


**Figure 5.** Electric field distribution.

The electric field polarizes the boundaries highlighted in blue in figure 6. The surface charge induced locally in any surface equals the norm of the electric displacement ( $D$ ) as<sup>6</sup>:

$$\sigma = \epsilon E = D. \quad (1)$$

The force per unit area  $f$  originated from the pull of the field in the induced charge is:

$$f = \sigma E = \epsilon E^2 = D \cdot E \quad (2)$$

The components of  $f$  can be written as:

$$f_x = E_x |D| \quad \text{and} \quad (3)$$

$$f_y = E_y |D|, \quad (4)$$

where  $E_x$  and  $E_y$  are the components of the field and  $|D|$  is the norm of the electric displacement.

Observations:

- In electrostatics simulations, convex geometries with discontinuous derivative cause the electric field to diverge in the vicinity of the discontinuity (power of points effect). So, to avoid spikes of electric field in figure 5 we rounded all convex edges.
- The characteristic time of charging and discharging the CMUT is much smaller than the operation frequency intended for this device, hence there is no phase difference between the applied voltage from equation (1) and the voltage in the plates. This is why we can use the *Electrostatics* module, otherwise, we should use the *Electric Currents* module.

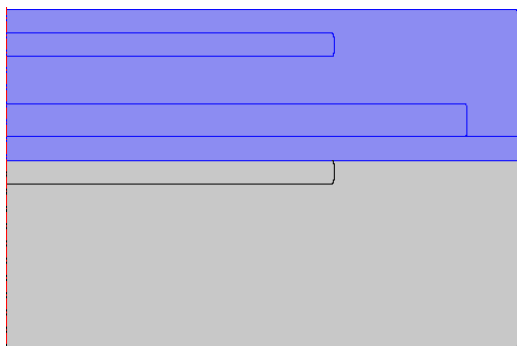
## 2.2 Solid Mechanics

As in the *Electrostatics*, the *Solid Mechanics* need not to be applied in all domains, just the ones that will deform under the electrostatic

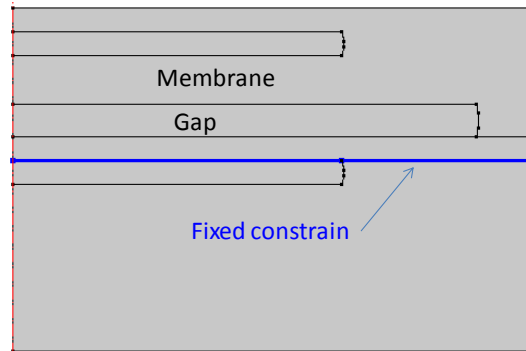
forces. Figure 6 shows the domains highlighted in blue where it is pertinent to apply the *Solid Mechanics*. Figure 7 highlights the bottom boundary with *fixed constrain* condition. As a good approximation, this boundary won't deform. Figure 8 shows the *Boundary load* condition, where the pressure given by eqs. (4) and (5) is applied. Compare with figure 5 and note that these are the only moving boundaries (on the membrane) embedded in electric field to be polarized. So, although the electric forces acts on every boundary, figure 8 shows the only ones that will contribute to move the membrane. The resulting stress in the CMUT is shown in figure 9. The solution in the vacuum gap was occulted, because it doesn't have a physical meaning.

Observations:

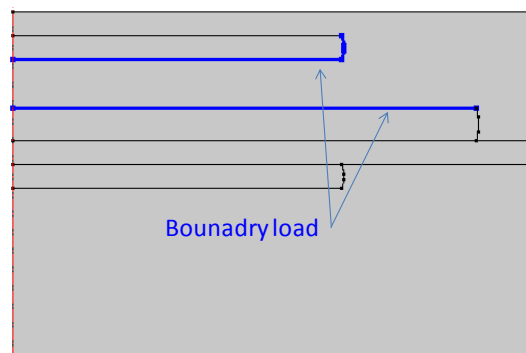
- The vacuum cavity in the CMUT must not have Young module null, so we simulate it with a mere 1 kPa. This value is negligible to influence the dynamics of the system and avoid errors in the solver
- Similarly to what happens in electrostatics, in solid mechanics discontinuities in the derivative of the geometry cause the stress to diverge in the vicinity of concave discontinuities (crack propagation effect). So, we rounded all concave corners to avoid ill behaved solutions.



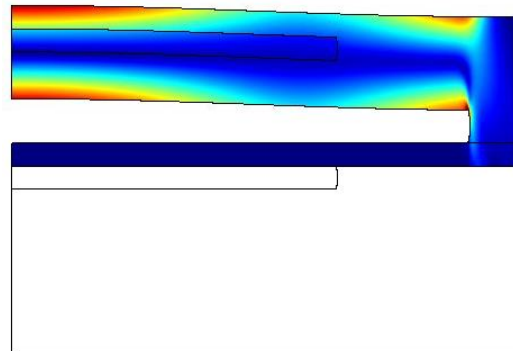
**Figure 6.** In blue, the domains where *Solid mechanics* applies.



**Figure 7.** No deformation boundary ( $dx=dy=0$ ).



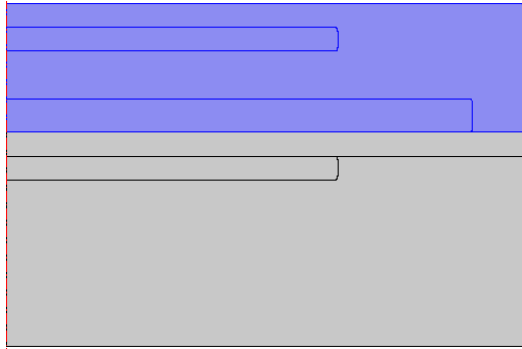
**Figure 8.** In blue, the boundaries with *Boundary load* condition that drives the deformation of the membrane.



**Figure 9.** Von Mises Stress distribution in the CMUT.

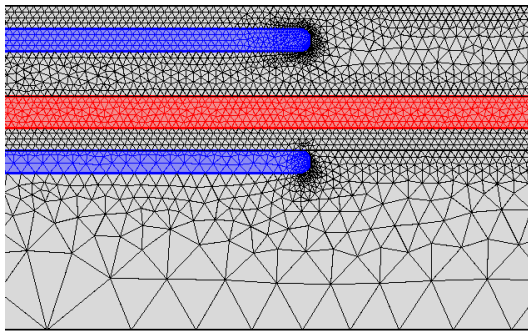
### 2.3 Moving Mesh

Figure 10 shows the domains where the *Moving Mesh* module is active. The Prescribed Mesh Displacement in the domains have components  $(u,v)$  which are the results from the *Solid Mechanics*. There are no BCs applicable to the boundaries.



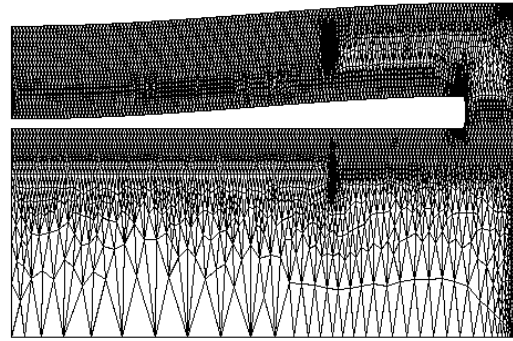
**Figure 10.** In blue, the domains where *Moving Mesh* applies.

Figure 11 shows the mesh generated. In this figure, the aspect ratio is restored, so just a short segment of the width is seen. The blue and red regions are highlighted to help visualize the components where the mesh concentrates. As usual, regions with large curvature are more densely meshed. In the bottom of the substrate the gradient of all variables are small, thus the mesh can be sparse.



**Figure 11.** Mesh in the CMUT.

The *Moving Mesh* feature allows elements to follow the deformation of the geometry. In figure 12 the deformed mesh is visible in a particular time. In this particular situation the separation of the membrane and the substrate is smaller. As a consequence, the electric force, the space charge and the deformation itself are all different then it would be if the mesh was fixed. As the mesh deforms, all variables are recalculated iteratively until they converge within the tolerance.



**Figure 12.** Deformed mesh in a particular time.

### 3 Results

An eigenfrequency study was made to determine, approximately, the first natural frequencies. Figure 13(a) and (b) shows the two first natural frequencies of the system. However, the eigenfrequency analysis does not account for the moving mesh and the corresponding corrections that should accompany the deformation. Therefore, the solution shown is just an approximation.

Knowing where the first resonance is, allows us to do a *Time dependent* analysis for frequencies as close to the resonance as possible. As we approach the resonance the higher will be the amplitude of oscillation and eventually the membrane will strike the substrate at 5.38 MHz, destroying the device. So, this is a situation to avoid in the real devices.

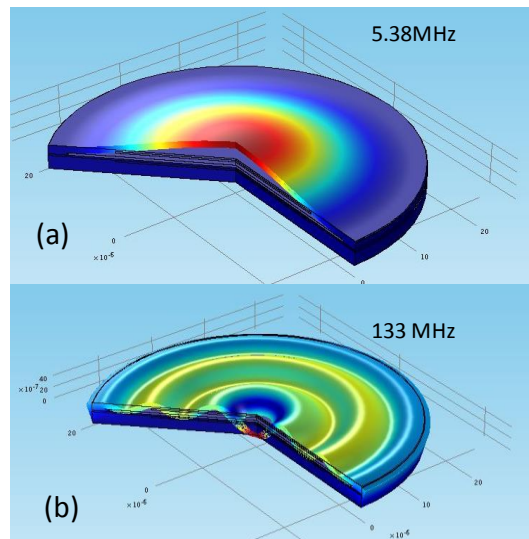


**Figure 13.** First two resonances of the system. In (a) 5.38MHz and in (b) 133MHz.

The time evolution allows us to track if the simulation is performing as expected. We spanned 3 periods to certify that the membrane was not collapsing on the substrate. Figure 3 shows the time evolution of the spacing between membrane and substrate for several frequencies. As the frequency approaches the resonance the amplitude increases until the gap eventually collapses. The time evolution presents some modulation due to the difference between the natural frequency of the device (5.3 MHz) and the excitation frequency shown in the inset. It can be seen that the closer the frequency is to the resonance the higher is the amplitude and the lower is the modulation frequency as expected.

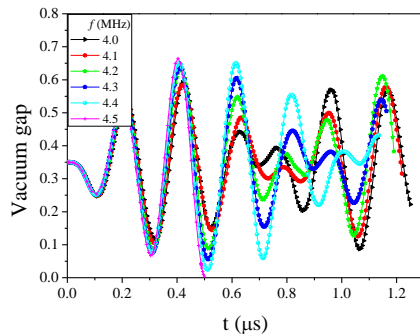


**Figure.13.** Time evolution of the CMUT in the first 5 periods near first resonance.

## Conclusion

We managed to obtain all the electric and structural characteristics of the device via simulation. Now we are prepared to step forward and study the configuration of maximum efficiency by analyzing the acoustic power transferred to the surrounding medium and to optimize the geometry that provides the maximum efficiency.

## Acknowledgements

The first author is thankful to the Brazilian Council of Scientific and Technological Development (CNPq) for the financial support; grant number 382634/2014-4.

## References

- <sup>1</sup> <http://www-kyg.stanford.edu/khuriyakub/opencms/en/research/cmuts/general/index.html>;
- <http://www.ieee-uffc.org/main/awards/outpapers/t02B1596.pdf>.
- <sup>2</sup> <http://en.wikipedia.org/wiki/CMOS>.
- <sup>3</sup> <http://www.youtube.com/watch?v=RhMUGTjbv4g>.
- <sup>4</sup> <http://www.youtube.com/watch?v=UKf0offCyw0>.
- <sup>5</sup> [http://en.wikipedia.org/wiki/Lift-off\\_\(microtechnology\)](http://en.wikipedia.org/wiki/Lift-off_(microtechnology)).
- <sup>6</sup> J. R. Reits, F. J. Milford, R.W. Christy, “Foundations of Electromagnetic Theory”.